Proceedings of the ASME 2017 36th International Conference on Ocean, Offshore and Arctic Engineering
OMAE2017
June 25-30, 2017, Trondheim, Norway

OMAE 2017-*****

TIME DOMAIN MODELLING OF FREQUENCY DEPENDENT WIND AND WAVE FORCES ON A THREE-SPAN SUSPENSION BRIDGE WITH TWO FLOATING PYLONS USING STATE SPACE MODELS

Yuwang Xu*
Department of Structural Engineering, Norwegian University of Science and Technology, Trondheim, Norway
yuwang.xu@ntnu.no

Ole Øiseth
Department of Structural Engineering, Norwegian University of Science and Technology, Trondheim, Norway
ole.oiseth@ntnu.no

Torgeir Moan
Centre for Ships and Ocean Structures (CeSOS), Norwegian University of Science and Technology, Trondheim, Norway
torgeir.moan@ntnu.no

ABSTRACT
Floating suspension bridges, one of several new designs to make it possible to cross deep and wide fjords, consist of three spans and supported by two tension leg platforms and two fixed traditional concrete pylons. Geometric nonlinearities, nonlinear aerodynamic and hydrodynamic forces and nonlinear mooring systems can become of high importance. Time domain methods are commonly applied when nonlinearities need to be considered. The main challenge in time domain simulation of the floating suspension bridge is the modelling of frequency-dependent aerodynamic self-excited forces and hydrodynamic radiation forces. This paper shows how rational functions fitted to aerodynamic derivatives and hydrodynamic added mass and potential damping can be converted to state space models to transform the frequency-dependent forces to time-domain. A user element is implemented in the software ABAQUS to be able to include the self-excited forces in the dynamic analysis. The element is developed as a one node element that is included in the nodes along the girder and the tension leg platforms. The responses of the floating suspension bridge under turbulent wind forces and first-order wave excitation forces are calculated in a comprehensive case study and compared with results obtained using a multi-mode frequency domain approach to illustrate the performance of the presented time-domain methodology.

Keywords: Suspension bridge, floating bridge, state space method

INTRODUCTION
In Norway, all ferries along the coastal highway E39 are aimed to be eliminated and replaced by bridges. Bjørnafjorden has a width of up to 5 km and depth of 500 m, which requires a significant extension of present bridge technology. A three span suspension bridge with two floating pylons is one of the new concepts considered to cross these wide and deep fjords [1, 2]. The bridge represents an entirely new design and it is a combination of offshore and bridge technologies, making very detailed analysis of its dynamic behavior necessary. One of the concerns is that large length-width ratio may induce serious nonlinear behavior. Thus, it is strongly recommended to apply time domain methods to investigate the importance of nonlinear effects.

One of the main challenges in the time domain simulations is to model the frequency dependent terms, i.e., aerodynamic damping and stiffness and hydrodynamic added mass and damping coefficients. An attractive alternative is to apply quasi-steady theory to model the aerodynamic self-excited forces and to model the added mass and the potential damping from the interaction with water in a simplified manner by picking values at a selected frequency, for instance the peak in the wave spectra. This makes the coefficients in the load models frequency independent such that they can be used in a straightforward manner in time domain. It can however be challenging to model the self-excited forces accurately using these simplified approaches, which has resulted in a number of suggestions for improvements, for instance, using convolution integrals or indicial functions [3-6] to simulate the fluid memory effect. To guarantee both computational accuracy and efficiency, state space models [7-12] are also commonly used in the modelling of the hydrodynamic and aerodynamic self-excited forces.

There exists very few studies about the performance of the state space methodology in the analysis of dynamic behavior of structures subjected to both wind and wave actions. A brief introduction to state space modelling of self-excited aerodynamic and radiation forces are therefore given in this paper. The reliability of the time domain method is verified through a comparison of critical wind velocity and dynamic response for a linearized system with frequency domain results.

*Corresponding author

FIGURE 1. A THREE-SPAN SUSPENSION BRIDGE WITH TWO FLOATING PYLONS. ILLUSTRATED BY ARNE JØRGEN MYHRE, STATENS VEGVESEN

EQUATION OF MOTION

The three-span suspension bridge with two floating pylons is shown in Fig. 1. Accounting for the wind and wave loading acting on the girder and pylons, the equation of motion can be expressed as:

$$\begin{aligned}\mathbf{M}_s\ddot{\mathbf{u}}(\mathrm{t})+\mathbf{C}_s\dot{\mathbf{u}}(t)+(\mathbf{K}_s+\mathbf{K}_h)\mathbf{u}(t)\\ =\mathbf{F}_{Wind,ex}(\mathrm{t})+\mathbf{F}_{se}(\mathrm{t})+\mathbf{F}_{Wave,ex}(\mathrm{t})-\mathbf{F}_{Rad}(\mathrm{t})\end{aligned} \quad (1)$$

Here, $\mathbf{M}_s$, $\mathbf{C}_s$ and $\mathbf{K}_s$ are the still-air mass, damping and stiffness matrices, respectively and $\mathbf{u}$ is displacement of the finite element model. The wind actions consist of wind forces $\mathbf{F}_{Wind,ex}$ due to the mean and turbulent wind velocity and self-excited force $\mathbf{F}_{se}$ which is generated by the motion of the structure. The hydrodynamic contributions consist of wave excitation forces $\mathbf{F}_{Wave,ex}$, the radiation forces $\mathbf{F}_{Rad}$ and the hydrostatic restoring stiffness $\mathbf{K}_h$. In this paper, only the theory about modelling the motion induced forces in an efficient manner in time domain is introduced. A brief overview of how the motion induced forces can be modeled by means of state space models is presented below while more details can be found in [13]. A detailed explanation of how the wave excitation forces and the buffeting wind forces are obtained by mean of Monte Carlo simulations is given in [13].

Modelling of radiation forces

Radiation forces are induced by the motion of the submerged part of the structure and consist of two components which are in phase with oscillation acceleration and velocity, respectively [14]. For a single frequency motion, it can be written as

$$\mathbf{F}_{Rad}=\mathbf{M}_h(\omega)\ddot{\mathbf{u}}+\mathbf{C}_h(\omega)\dot{\mathbf{u}} \quad (2)$$

Here $\mathbf{M}_h(\omega)$ and $\mathbf{C}_h(\omega)$ are the frequency dependent added mass and potential damping matrices. When the oscillation frequency goes to infinity, the damping coefficient converges to zero, whereas the added mass becomes constant and frequency independent.

$$\begin{aligned}\mathbf{M}_h(\omega)&=\mathbf{m}_h(\omega)+\mathbf{M}_h(\infty)\\ \mathbf{C}_h(\omega)&=\mathbf{c}_h(\omega)+\mathbf{C}_h(\infty)=\mathbf{c}_h(\omega)\end{aligned} \quad (3)$$

The constant part of the added mass is convenient to model in the dynamic response analysis because it can be directly added in the mass matrix in the equation of motion. Only accounting for the frequency dependent terms, the radiation forces can be expressed in frequency domain as:

$$\mathbf{G}_{\mathbf{z}_{Rad}}(\omega)=\mathbf{H}(\omega)\mathbf{G}_{\dot{\mathbf{u}}}(\omega) \quad (4)$$

Here, $\mathbf{G}_{\mathbf{z}_{Rad}}(\omega)$ and $\mathbf{G}_{\dot{\mathbf{u}}}(\omega)$ are the Fourier transform of the radiation force and the velocity of the submerged structure which is considered as a rigid body in the hydrodynamic analysis. $\mathbf{H}(\omega)$ denotes the hydrodynamic transfer function $\mathbf{H}(\omega)=i\omega\mathbf{m}_h(\omega)+\mathbf{c}_h(\omega)$. By applying the inverse Fourier transform to Eq. (4), the forces can be expressed in the time domain as a convolution integral:

$$\mathbf{z}_{Rad}(\mathrm{t})=\int_{-\infty}^{\infty}\mathbf{h}(\mathrm{t}-\tau)\dot{\mathbf{u}}(\tau)d\tau \quad (5)$$

Here $\mathbf{h}(\mathrm{t})$ is the inverse Fourier transform of $\mathbf{H}(\omega)$. Equation (5) consists of $6\times6=36$ convolution integrals and as noted by several authors [10, 11], it is very time-consuming to solve the convolution integrals during a dynamic analysis. Replacing them by state-space models is an efficient alternative. In this chapter we will only present the expression of the convolution integral giving contribution to the radiation force in direction *i* due to motion in direction *j*, $z_{ij}^{(Rad)}(\mathrm{t})=\int_{-\infty}^{\infty}h_{ij}(t-\tau)\dot{u}_j(\tau)\,\mathrm{d}\tau$ since the others are handled in the same manner. Convolution is a linear operator, and it is well known that this can be modelled by means of state space models, see [11] for further details. The radiation force in direction *i* due to motion in direction *j* can thus be expressed as

$$\begin{cases}\dot{\mathbf{X}}(\mathrm{t})=\mathbf{D}_c^{(\mathrm{H})}\mathbf{X}(\mathrm{t})+\mathbf{E}_c^{(\mathrm{H})}\dot{u}_j(\mathrm{t})\\ z_{ij}^{(Rad)}(\mathrm{t})=\mathbf{Q}_c^{(\mathrm{H})}\mathbf{X}(\mathrm{t})\end{cases} \quad (6)$$

See [11, 13] for detail derivation of Eq. (6) and the content of the constant matrices $\mathbf{D}_c^{(\mathrm{H})}$, $\mathbf{E}_c^{(\mathrm{H})}$ and $\mathbf{Q}_c^{(\mathrm{H})}$.

Modelling of aerodynamic self-excited forces

Similar to the radiation forces presented in Eq. (4), the aerodynamic self-excited forces $\mathbf{q} = \begin{bmatrix} q_y & q_z & q_\theta \end{bmatrix}^T$ can be expressed in frequency domain as follows:

$$\begin{aligned} \mathbf{G}_q(\omega) &= (i\omega \mathbf{C}_{ae}(\omega) + \mathbf{K}_{ae}(\omega))\mathbf{G}_u(\omega) \\ &= \mathbf{F}(\omega)\mathbf{G}_u(\omega) \end{aligned} \tag{7}$$

Here, $\mathbf{G}_q(\omega)$ and $\mathbf{G}_u(\omega)$ are the Fourier transform of self-excited forces and displacements. Their positive directions are displayed in Fig. 2. The aerodynamic damping matrix, $\mathbf{C}_{ae}(K)$, and the aerodynamic stiffness matrix, $\mathbf{K}_{ae}(K)$, contain 18 aerodynamic derivatives, P_n^*, H_n^* and A_n^*, $n \in \{1,2,...,6\}$, which are functions of the reduced frequency of motion $K = (B\omega)/V$ [15].

$$\mathbf{C}_{ae} = \frac{1}{2}\rho V K B \begin{bmatrix} P_1^* & P_5^* & BP_2^* \\ H_5^* & H_1^* & BH_2^* \\ BA_5^* & BA_1^* & B^2A_2^* \end{bmatrix},$$

$$\mathbf{K}_{ae} = \frac{1}{2}\rho V^2 K^2 \begin{bmatrix} P_4^* & P_6^* & BP_3^* \\ H_6^* & H_4^* & BH_3^* \\ BA_6^* & BA_4^* & B^2A_3^* \end{bmatrix}$$

Here, V is the mean wind velocity, ρ is the air density, and B is the width of the girder. The aerodynamic derivatives are commonly determined using wind tunnel tests [16].

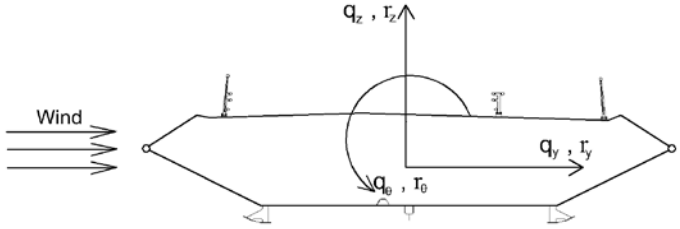

FIGURE 2. AERODYNAMIC FORCES ACTING ON THE BRIDGE SECTION CONSIDERED IN THIS STUDY

By applying the inverse Fourier transform to Eq. (7), the self-excited forces in time domain can be expressed as follows:

$$\mathbf{q}(\mathrm{t}) = \int_{-\infty}^{\infty} \mathbf{f}(\mathrm{t}-\tau)\mathbf{u}(\tau)d\tau \tag{8}$$

Here, $\mathbf{f}(\mathrm{t})$ and $\mathbf{u}(\mathrm{t})$ are the inverse Fourier transforms of $\mathbf{F}(\omega)$ and $\mathbf{G}_u(\omega)$.

Integrating the distributed self-excited forces applying the principle of virtual work and introducing the state space model to replace the convolution integrals render the following expression for the nodal self-excited forces:

$$\begin{cases} \mathbf{F}_{se} = \mathbf{A}_1\mathbf{u}(\mathrm{t}) + \mathbf{A}_2\dot{\mathbf{u}}(\mathrm{t}) + \mathbf{z}_{se}(\mathrm{t}) \\ \dot{\mathbf{X}}(\mathrm{t}) = \mathbf{D}_c^{(ae)}\mathbf{X}(\mathrm{t}) + \mathbf{E}_c^{(ae)}\dot{\mathbf{u}}(\mathrm{t}) \\ \mathbf{z}_{se}(\mathrm{t}) = \mathbf{Q}_c^{(ae)}\mathbf{X}(\mathrm{t}) \end{cases} \tag{9}$$

See [10, 13] for detail derivation of Eq. (9) and expression for the constant matrices $\mathbf{A}_1$, $\mathbf{A}_2$, $\mathbf{D}_c^{(ae)}$, $\mathbf{E}_c^{(ae)}$ and $\mathbf{Q}_c^{(ae)}$.

Implementation in ABAQUS

Inserting Eqs. (2), (6) and (9) into Eq. (1), it is found that the self-excited force in time domain includes five terms: $\mathbf{M}_h(\infty)\ddot{\mathbf{u}}$, $\mathbf{A}_2\dot{\mathbf{u}}$ $\mathbf{A}_1\mathbf{u}$, $\mathbf{z}^{(se)}$ and $\mathbf{z}^{(Rad)}$. The last two terms are more complicated because they depend on the motion history and need to be modelled by the state space models outlined above. A user element is then implemented in ABAQUS in order to include these terms in the dynamic analysis [17]. The element is developed as a one node element and is modelled on top of the nodes of ordinary beam elements such that it is not necessary to involve the mass, damping and stiffness terms related to the structure. Details can be found in [13].

STABILITY OF THE SYSTEM

It is of crucial importance to study the stability and the damping of the dynamic system before conducting time domain simulations since the fluid-structure interaction effects will change the properties of the dynamic system. The interaction with water will provide stiffness due to buoyancy, potential damping and added mass. The interaction with the wind is somewhat more complicated since the aerodynamic stiffness and damping forces is strongly influenced by the mean wind velocity. Flutter is one of the most important concerns when designing cable-supported bridges since this may lead to a collapse like the infamous Tacoma Narrows Bridge. A multimode approach is commonly used when studying the stability of cable-supported bridges and this approach will also be used in this paper [18]. The first step is to establish a comprehensive finite element model of the bridge and calculate the still-air and dry natural frequencies and modes. In our case it is a good idea to include the restoring stiffness as well as the added mass when the frequency goes to infinity since these effects will change the modes and frequencies severely. The next step is to use the resulting modes as assumed shapes to establish a generalized equation of motion and include the rest of the fluid structure interaction effects. This will couple the equation of motion, which implies that the stability of the system can be studied by considering the complex eigenvalues of the new equation of motion. The characteristic equation of motion can be defined as

$$\begin{aligned} &s^2\left(\tilde{\mathbf{M}}_0 + \tilde{\mathbf{M}}_h(\omega)\right) + s\left(\tilde{\mathbf{C}}_0 + \tilde{\mathbf{C}}_h(\omega) - \tilde{\mathbf{C}}_{ae}(\mathrm{V},\omega)\right) \\ &+ \left(\tilde{\mathbf{K}}_0 + \tilde{\mathbf{K}}_h - \tilde{\mathbf{K}}_{ae}(\mathrm{V},\omega)\right) = 0 \end{aligned} \tag{10}$$

Here $s = a + i\omega$ denotes the eigenvalues of the system while $\tilde{\mathbf{M}}_0$, $\tilde{\mathbf{C}}_0$ and $\tilde{\mathbf{K}}_0$ represents the generalized still-air and dry

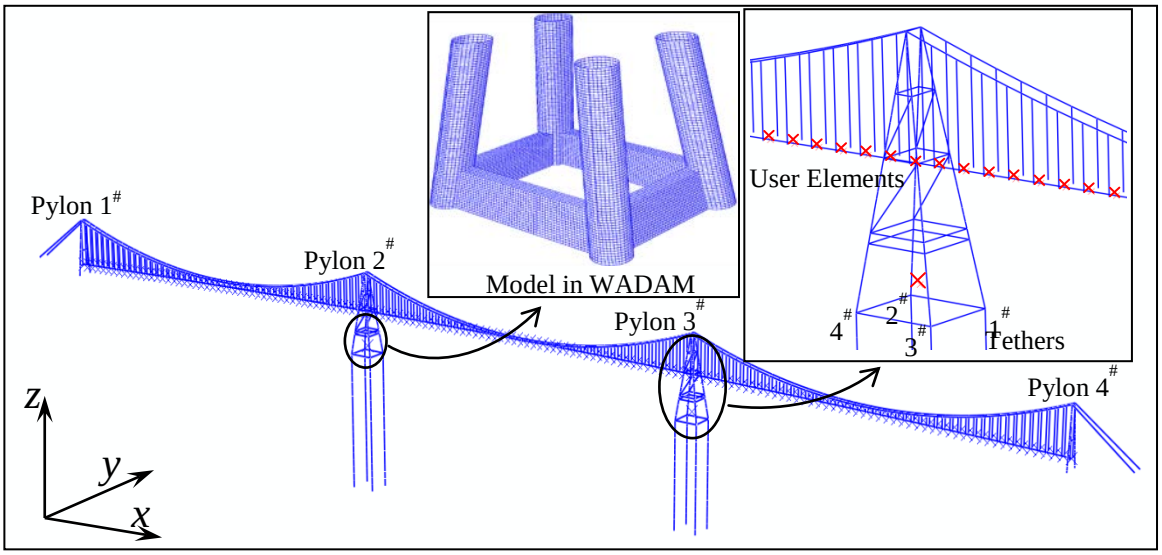

FIGURE 3. FINITE ELEMENT MODEL OF THE THREE-SPAN SUSPENSION BRIDGE WITH TWO FLOATING PYLONS

mass, damping and stiffness matrix respectively. The aerodynamic effects are introduced by the generalized aerodynamic stiffness matrix $\tilde{\mathbf{K}}_{ae}(\mathrm{V},\omega)$ and damping matrix $\tilde{\mathbf{C}}_{ae}(\mathrm{V},\omega)$ that are defined in terms of aerodynamic derivatives, which are functions of the mean wind velocity and the frequency of motion. The hydrodynamic effects are introduced by the frequency dependent added mass $\tilde{\mathbf{M}}_h(\omega)$, potential damping $\tilde{\mathbf{C}}_h(\omega)$ matrices, as well as the constant restoring stiffness $\tilde{\mathbf{K}}_h$. The eigenvalue problem defined in Eq.(10) needs to be solved in an iterative manner since many of the matrices involved contain terms that are function of the frequency of motion. The stability of the combined structure and flow system can be studied by considering the real part of the eigenvalues since the damping ratios of the system is obtained by $\xi_i = -\mathrm{Re}(\mathrm{s}_i)/|s_i|$.

NUMERICAL SIMULATIONS

This paper is mainly focused on the verification of the time domain method. Some properties of the bridge are referred to Hardanger bridge, one of the slenderest bridge in Norway, because the detailed design parameters of the new bridge were not available when the study was started. Fig. 3 shows the finite element model used for dynamic analysis in ABAQUS as well as the panel model used to calculate the hydrodynamic force in WADAM [19]. The three main spans of the bridge are 1385 m long and the top of the pylons is approximately 200 m above the mean water level. The water depth is 550 m and 450 m at the left and right floating pylons, whereas the draft of both pylons is approximately 65 m. The girder, main cable, tethers, hangers and pylons are modelled using the beam elements in ABAQUS. The aerodynamic self-excited and hydrodynamic radiation forces are simulated by implementing a user element. The element is developed as a one-node element in the nodes of the girder and the gravity center of the submerged part of the floating pylons as illustrated by the red markers in the figure. The added mass, potential damping and first order transfer functions for the wave excitation forces are obtained using the potential theory in WADAM. To obtain accurate hydrodynamic forces, the geometry of the submerged part of the pylon in WADAM must be modelled in an identical manner to the actual one instead of being simplified to a beam.

Flutter analysis based on the multi-mode method

Several vibration modes of the system are displayed in Fig. 4. It is important to keep in mind that the modes have been obtained including only added mass when the frequency goes to infinity and the restoring stiffness, which implies that many of the frequencies and corresponding modes will change when the rest of the hydrodynamic effects are added together with the aerodynamic self-excited forces. This effect will be accurately captured if sufficient generalized coordinates are included in the analysis. The vibration modes are in general more complicated than what are typically seen for cable-supported bridges, making the flutter analysis more complicated. This is partly because the bridge has three spans and partly because of the floating pylons. The flutter stability limit considering both aerodynamic and hydrodynamic contributions is V_{cr}=74.96 m/s and ω_{cr}=1.63 rad/s.

Flutter analysis based on the time-domain method

It is also of interest to study the free vibration response of the system close to the critical velocity in time domain in order to compare it with the multi-modal approach to validate its performance. At the start of the time-domain simulation, an impulsive loading is imposed at the mid-span of the bridge. Time series of the torsional response at the mid-span of the

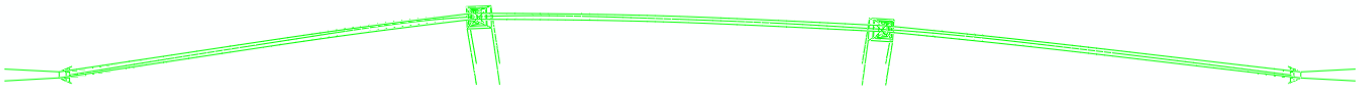

a) Mode 1, natural frequency: 0.0727 rad/s, lateral motion of superstructure

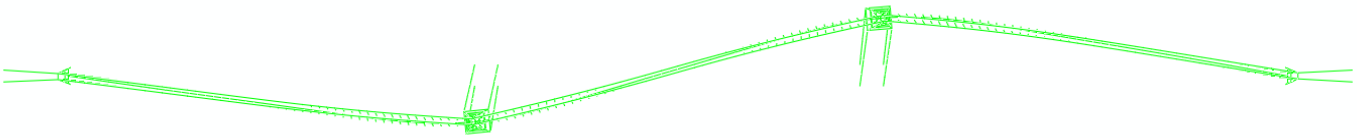

b) Mode 2, natural frequency: 0.0967 rad/s, lateral motion of superstructure

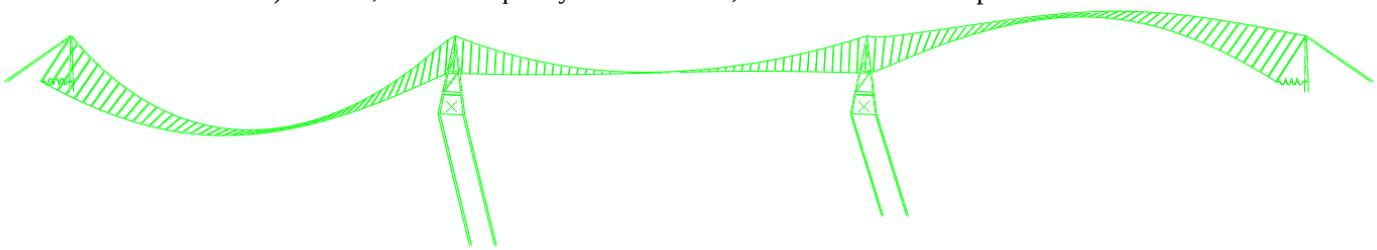

c) Mode 3, natural frequency: 0.185 rad/s, vertical motion of superstructure, surge and pitch of floating pylons

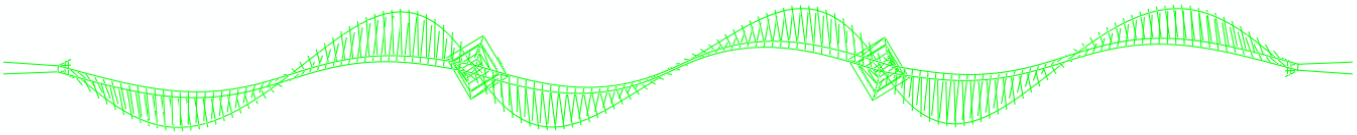

d) Mode 7, natural frequency: 0.462 rad/s, lateral motion of superstructure, yaw of floating pylons, torsional motion of the girder

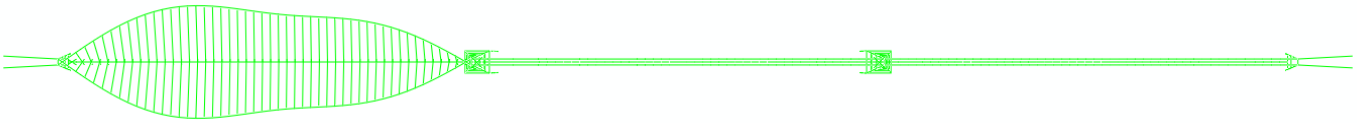

e) Mode 19, natural frequency: 0.913 rad/s, deformation of the cable

FIGURE 4. THE NATURAL MODE SHAPES OF THE SUSPENSION BRIDGE WITH TWO FLOATING PYLONS. ONLY ADDED MASS WHEN THE FREQUENCY GOES TO INFINITY AND THE HYDROSTATIC RESTORING STIFFNESS ARE CONSIDERED.

bridge are displayed in Fig. 5 at a mean wind velocity of 70, 74 and 75 m/s. As can be seen from the figure, the damping is very low at 74 m/s while the damping appears to be zero or very close to zero at 75 m/s. The response at 76m/s is displayed in Fig. 6 and the response has a clear divergent nature. A snapshot of the structure showing the response around 2500 seconds is displayed in Fig. 7. Contribution from all modes besides the flutter vibration modes has been damped out making the snapshot a visualization of the flutter vibration mode. The mode will in general be complex and thus slightly time dependent but the snapshot gives an overall good representation of the motions seen in the animation of the response. As the figure illustrates it is mainly the girder, hangers and the two main cables that participate in the flutter motion while only small motions can be observed for the floating pylons.

Dynamic response for the linearized system

When the system is linear, the time domain method introduced in this paper should result in the same response as the frequency domain approach if a sufficient amount of generalized coordinates is included in the modelling. Therefore, both time domain and frequency domain methods are applied to predict the dynamic response of the floating suspension bridge at a mean wind velocity of 35 m/s and significant wave height of 4.88 m in order to verify the reliability of the method. Turbulent wind forces that act on the pylon have not been considered.

The mean value of the standard deviation of the displacement along the girder for 5 time-domain simulations of 1-hour

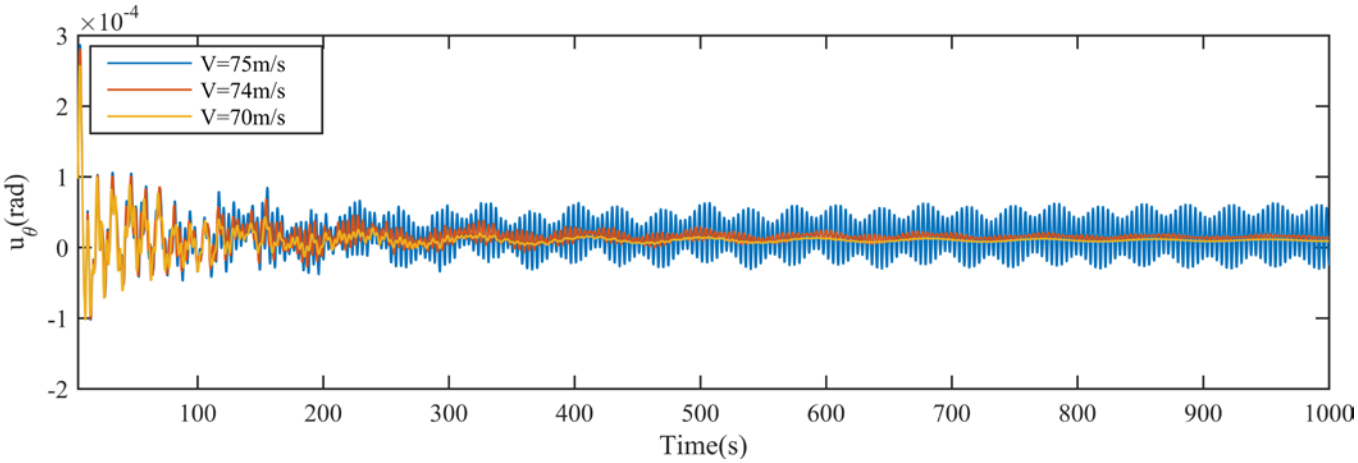

FIGURE 5. TORSIONAL RESPONSE AT MID-SPAN UNDER DIFFERENT MEAN WIND VELOCITIES

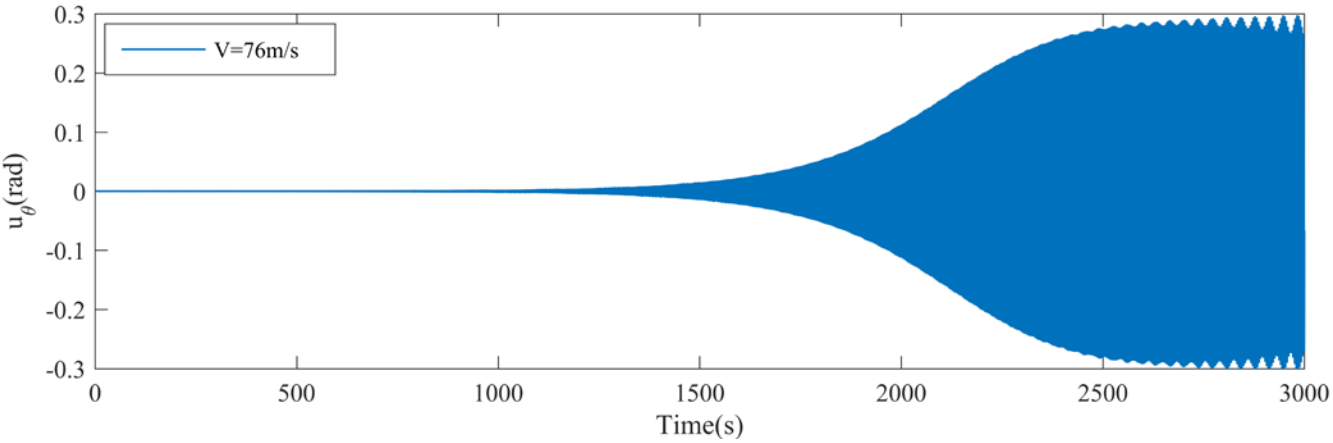

FIGURE 6. TORSIONAL RESPONSE AT MID-SPAN UNDER MEAN WIND VELOCITIES OF 76 M/S

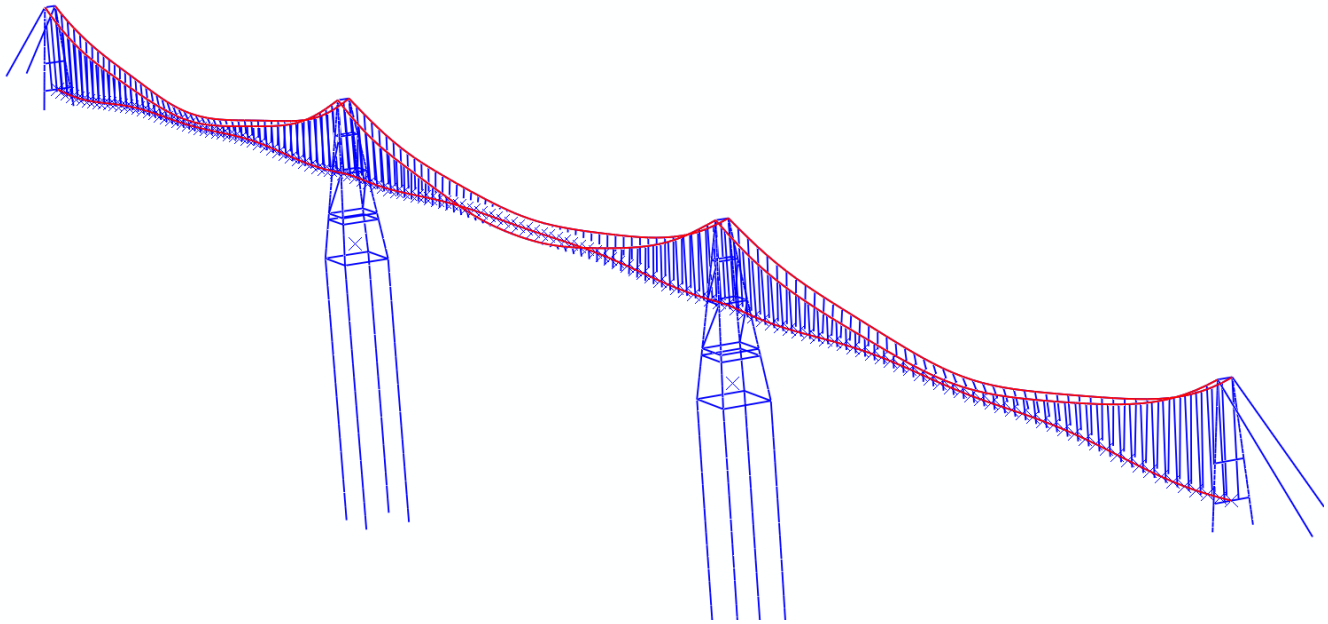

a)

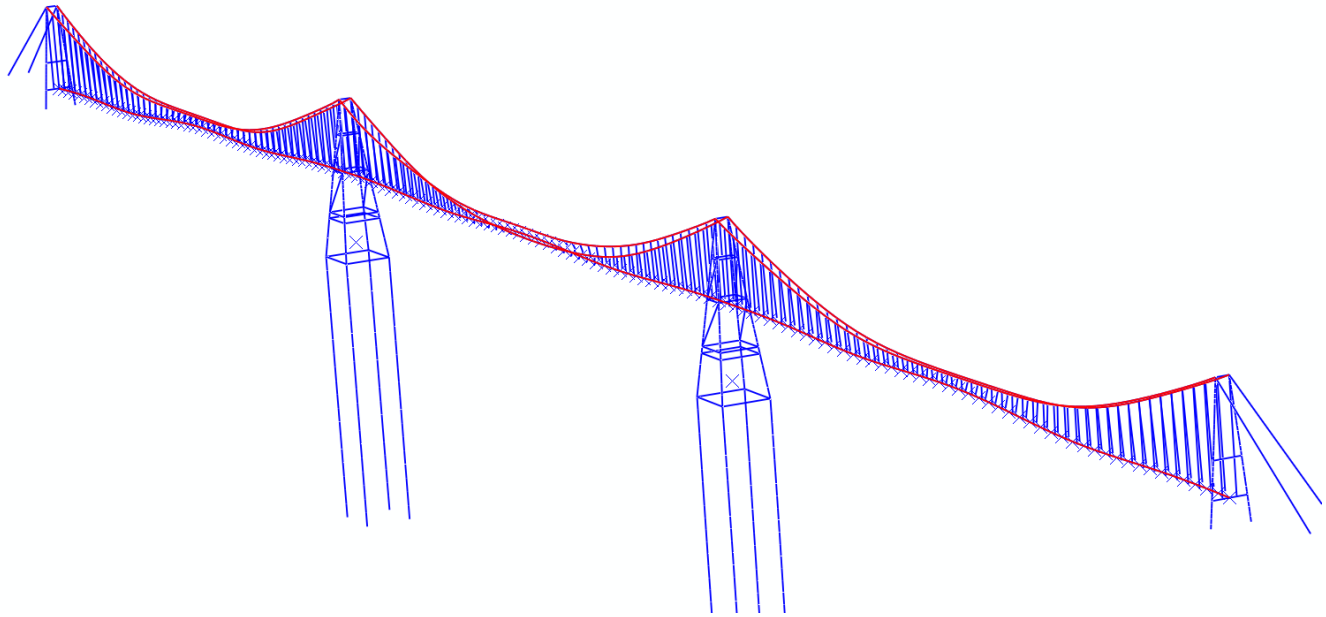

b)

FIGURE 7. A SNAPSHOT OF THE STRUCTURE AT 2500 S AND 2501.8 S UNDER MEAN WIND VELOCITIES OF 76 M/S. THE PERIOD OF THE FLUTTER RESPONSE IS APPROXIMATELY 3.87 S. THE RED LINES ARE USED TO MAKE THE GIRDER AND CABLE EASIER TO RECOGNIZE. DEFORMATION SCALE FACTOR IS 5. A) T=2500 S; B) T=2501.8 S

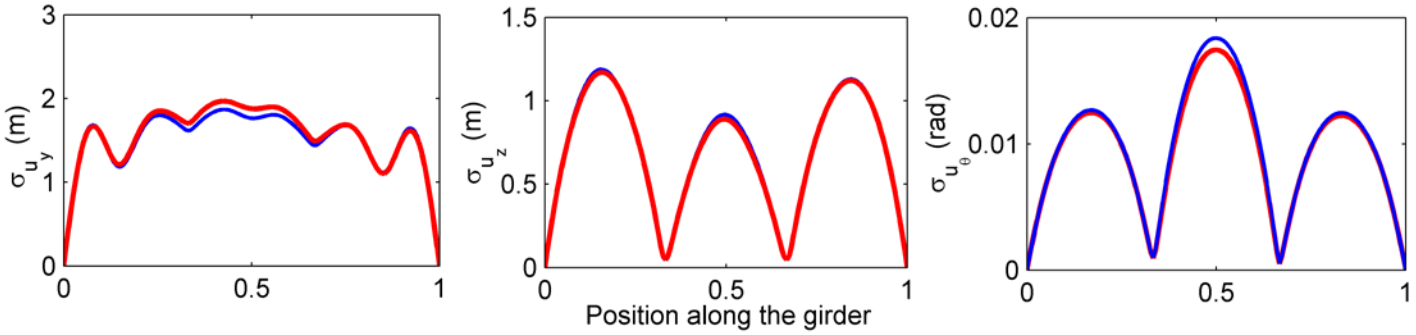

FIGURE 8. THE STANDARD DEVIATIONS OF THE DISPLACEMENT ALONG THE GIRDER IN LATERAL, VERTICAL AND TORSIONAL DIRECTION. THE SOLID RED LINE — IS THE AVERAGE OF THE 5 REALIZATIONS WHILE THE SOLID BLUE LINE — REPRESENTS THE FREQUENCY DOMAIN RESULTS.

TABLE 1. COMPARISON OF TIME AND FREQUENCY DOMAIN RESULTS OF THE STANDARD DEVIATION OF THE DISPLACEMENT RESPONSE FOR PYLON 2#

	Multi-Mode Method	Time Domain Method (mean value)	Difference (%)
σ_y (m)	1.61	1.70	5.53
σ_z (m)	4.53	4.83	6.47
σ_{θ_x} (x10^{-3} rad)	1.03	0.973	-5.78
σ_{θ_y} (x10^{-3} rad)	1.21	1.18	-1.5

duration is compared to frequency-domain results in Fig. 8. As can be seen, the results correspond very well along the entire girder. Table. 1 shows the variance of the displacement of the pylons obtained from time series based on time domain method and from response spectral density based on frequency domain method. The mean value corresponds well. Thus, the linearized time-domain simulations accurately capture the dynamic behavior. Moreover, the time domain approach allows for including nonlinear features, which is discussed in [13].

CONCLUSIONS

This paper focuses on the efficient modelling of the aerodynamic self-excited forces and hydrodynamic radiation forces on a three-span suspension bridge with two floating pylons using state space models.

Critical wind velocity and dynamic response for a linearized system was used to verify the presented time-domain methodology by comparing the obtained response statistics to the frequency domain results. The conclusion is that the time domain methodology can capture the dynamic behavior of the structure because the time- and frequency-domain results are consistent.

ACKNOWLEDGEMENTS

This study was conducted with financial support from the Norwegian Public Roads Administration. The authors gratefully acknowledge this support. The finite element model applied in this study was created by the two master students, Sondre Halden and Shun Wei Gong. Their effort is gratefully acknowledged.

REFERENCES

[1] Fredriksen AG, Bonnemaire B, Lie H, Munkeby J, Nesteby A, Buckholm P, et al. Comparison of Global Response of a 3-Span Floating Suspension Bridge With Different Floater Concepts. ASME 2016 35th International Conference on Ocean, Offshore and Arctic Engineering: American Society of Mechanical Engineers; 2016. p. V007T06A66-VT06A66.

[2] Veie J, Holtberget S. Three span floating suspension bridge crossing the Bjørnafjord. Multi-Span Large Bridges: International Conference on Multi-Span Large Bridges, 1-3 July 2015, Porto, Portugal: CRC Press; 2015. p. 373.

[3] Borri C, Costa C, Zahlten W. Non-stationary flow forces for the numerical simulation of aeroelastic instability of bridge decks. Computers & Structures 2002;80:1071-9.

[4] Cummins W. The impulse response function and ship motions. DTIC Document; 1962.

[5] Kashiwagi M. Transient responses of a VLFS during landing and take-off of an airplane. Journal of Marine Science and Technology 2004;9:14-23.

[6] Salvatori L, Spinelli P. Effects of structural nonlinearity and along-span wind coherence on suspension bridge aerodynamics: Some numerical simulation results. Journal of Wind Engineering and Industrial Aerodynamics 2006;94:415-30.

[7] Chen X, Matsumoto M, Kareem A. Time Domain Flutter and Buffeting Response Analysis of Bridges. Journal of Engineering Mechanics 2000;126:7-16.

[8] Fossen TI. A nonlinear unified state-space model for ship maneuvering and control in a seaway. International Journal of Bifurcation and Chaos 2005;15:2717-46.

[9] Kristiansen E, Hjulstad Å, Egeland O. State-space representation of radiation forces in time-domain vessel models. Ocean Engineering 2005;32:2195-216.

[10] Øiseth O, Rönnquist A, Sigbjörnsson R. Finite element formulation of the self-excited forces for time-domain assessment of wind-induced dynamic response and flutter stability limit of cable-supported bridges. Finite Elements in Analysis and Design 2012;50:173-83.

[11] Taghipour R, Perez T, Moan T. Hybrid frequency–time domain models for dynamic response analysis of marine structures. Ocean Engineering 2008;35:685-705.

[12] Taghipour R, Perez T, Moan T. Time-domain hydroelastic analysis of a flexible marine structure using state-space models. Journal of Offshore Mechanics and Arctic Engineering 2009;131:011603.

[13] Xu Y, Øiseth O, Moan T. Time domain simulations of wind and wave induced load effects for a three span suspension bridge with two floating pylons. . Submitted 2017.

[14] Faltinsen O. Sea loads on ships and offshore structures: Cambridge university press; 1993.

[15] Scanlan RH, Tomko J. Air foil and bridge deck flutter derivatives. Journal of Soil Mechanics & Foundations Div 1971.

[16] Diana G, Rocchi D, Belloli M. Wind tunnel: a fundamental tool for long-span bridge design. Structure and Infrastructure Engineering 2015;11:533-55.

[17] Hibbett, Karlsson, Sorensen. ABAQUS/standard: User's Manual: Hibbitt, Karlsson & Sorensen; 1998.

[18] Ge YJ, Tanaka H. Aerodynamic flutter analysis of cable-supported bridges by multi-mode and full-mode approaches. Journal of Wind Engineering and Industrial Aerodynamics 2000;86:123-53.

[19] Lee C-H. WAMIT theory manual: Massachusetts Institute of Technology, Department of Ocean Engineering; 1995.